

The Effect of Various Soil Hydraulic Property Estimates on Soil Moisture Simulations

Molly M. Gribb,* Irina Forkutsa, Aleshia Hansen, David G. Chandler, and James P. McNamara

Models of water movement in unsaturated soils require accurate representations of the soil moisture retention and hydraulic conductivity curves; however, commonly used laboratory methods and pedotransfer functions (PTFs) are rarely verified against field conditions. In this study, we investigated the effects of using soil hydraulic property information obtained from different measurement and estimation techniques on one-dimensional model predictions of soil moisture content. Pairs of time domain reflectometry waveguides and tensiometers were installed at two depths in the side of a soil pit face to obtain in situ measurements. Undisturbed soil samples were taken near the instruments and subjected to particle size analysis, multistep outflow (MSO), and falling-head permeability tests to obtain estimates of the soil moisture retention curves. Three scaling methods were then applied to improve the fit of the various estimates to the field data. We found that soil hydraulic property estimates obtained from inverse methods lead to the best simulations of soil moisture dynamics, and that laboratory MSO tests or commonly used PTFs perform poorly. These laboratory and PTF estimates can be dramatically improved, however, by simply constraining the range of possible moisture contents to the minimum and maximum measured in the field. It appears that this method of scaling PTF results can be used to obtain soil hydraulic property inputs of sufficient accuracy for plot-scale modeling efforts without requiring expensive laboratory or in situ tests.

ABBREVIATIONS: DOY, day of the year; MR, mean residual; MSO, multistep outflow; PTF, pedotransfer function; RB, Rawls and Brakensiek (1985); TDR, time domain reflectometry; WOE, Wösten et al. (1999).

HYDROLOGIC MODELS based on one-dimensional simulations of the vadose zone are routinely used to predict or study fluxes of moisture, solutes, and energy at field and watershed scales. For the results of these models to be useful, sufficiently accurate soil hydraulic property inputs, namely the soil moisture retention and hydraulic conductivity curves, $\theta(h)$ and $K(h)$, are needed. These properties can be estimated from laboratory and field experiments using direct measurements or inverse solution methods. These methods can be time consuming and expensive (Dane and Topp, 2002), however, and laboratory tests on small samples often don't reflect field behavior (Basile et al., 2003). Alternatively, PTFs allow users to estimate soil hydraulic properties from limited information such as soil texture, bulk density, and organic C quickly and cheaply (Wösten et al., 2001;

Pachepsky et al., 1996). Unfortunately, PTFs can yield results that do not adequately reflect field behavior.

Despite the shortcomings of laboratory tests and PTFs, many vadose zone modeling efforts rely on them because in situ measurements of soil hydraulic properties are typically not available. When such information is available, however, we can investigate how well these estimates of the soil hydraulic properties from laboratory tests and PTFs compare with in situ data and how the in situ information can be used to improve these estimates.

In this study, we investigated the effects of using the soil hydraulic properties obtained by differing measurement and estimation techniques on one-dimensional model predictions of soil moisture content in a small instrumented area within the Dry Creek Experimental Watershed, a nonagricultural, mountainous site near Boise, ID. The soil hydraulic properties were estimated from in situ measurements, laboratory MSO tests, four PTFs, and finally, by inversion of field pressure head and moisture content data from two short infiltration events using HYDRUS-1D (Šimůnek et al., 2005). The soil moisture retention curves resulting from these methods were compared with the curves derived from in situ data to determine how well the estimates reflect field behavior. Three scaling approaches were used in an attempt to improve the fit of the various estimated and predicted retention curves to the in situ data. The different hydraulic parameter sets were then used as inputs for HYDRUS-1D to determine the effects of different hydraulic property inputs on predictions of soil moisture at two depths and cumulative water flux out of the bottom of the soil profile for an extended simulation period.

M.M. Gribb, I. Forkutsa, and A. Hansen, Dep. of Civil Engineering, Boise State Univ., 1910 University Dr., Boise, ID 83725-2075; D.G. Chandler, Dep. of Civil Engineering, Kansas State Univ., Manhattan, KS 66506; and J.P. McNamara, Dep. of Geosciences, Boise State Univ., 1910 University Dr., Boise, ID 83725-1535. Received 27 Apr. 2008. *Corresponding author (mgribb@boisestate.edu).

Vadose Zone J. 8:321–331
doi:10.2136/vzj2008.0088

© Soil Science Society of America

677 S. Segoe Rd. Madison, WI 53711 USA.

All rights reserved. No part of this periodical may be reproduced or transmitted in any form or by any means, electronic or mechanical, including photocopying, recording, or any information storage and retrieval system, without permission in writing from the publisher.

Materials and Methods

Field Measurements

This study was conducted in the Treeline catchment in the Dry Creek Experimental Watershed near Boise, ID (Fig. 1). The Treeline catchment has a mean elevation of 1620 m, a relief of 35 m, and a northwest–southeast orientation with soil formed in place from weathering of the granitic bedrock. A meteorological station on the northeast-facing slope records precipitation, snow depth, air temperature, relative humidity, wind speed, wind direction, incoming solar radiation, net longwave radiation, soil temperature, and soil moisture on a CR10X datalogger (Campbell Scientific, Logan, UT). For detailed information about instrumentation of the site, refer to McNamara et al. (2005) and Williams et al. (2008).

Several soil pits were dug to the bedrock interface at 5- to 10-m intervals upslope from the stream in 2002 as part of a study to investigate hydraulic connections between hillslopes and streams. In the present study, we restricted the analysis to one-dimensional infiltration in one pit, SU10, to focus on soil hydraulic properties rather than hillslope hydrology. The naming convention indicates that the pit is on the south-facing slope, located 10 m above the stream.

At SU10, pairs of time-domain reflectometry (TDR) waveguides and tensiometers were installed horizontally at 15 and 52 cm below the ground surface into the side of the soil pit. The soil–bedrock interface was a few centimeters below the lowest sensor. The TDR100 waveguides were 30 cm in length; coaxial multiplexers and CR10X dataloggers (Campbell Scientific, Logan, UT) were used to collect hourly data. Errors in soil moisture measurements are difficult to quantify because, in addition to instrument accuracy, errors may arise from various site-specific conditions; however, TDR is considered to be among the best methods of in situ soil moisture measurement (Blonquist et al., 2005). Complementary measurements of soil water pressure head were made with automated tensiometers constructed from remote soil moisture samplers (Soil Moisture Equipment, Goleta, CA) and 34.47-kPa (5-psi, $\pm 0.2\%$ of full-scale output) differential pressure transducers (Sensym ASCX05DN, Honeywell, Morristown, NJ). Undisturbed soil samples (5.4 cm in diameter and 3 cm in length) were taken from each pit at the same depth as the instruments during installation, 20 to 50 cm away from the sensor pairs so as not to influence subsequent measurements. In 2005 and 2006, additional undisturbed soil cores were taken from new pits dug 100 cm away from the instrumented pit and at the approximate depths of the TDR–tensiometer pairs for MSO and saturated hydraulic conductivity (K_s) testing.

Laboratory Measurements

The original SU10 samples, and those taken later, were analyzed for particle size distribution via mechanical sieving and hydrometer analysis (ASTM, 2007). Three to five falling-head permeability tests (Reynolds et al., 2002) were performed on two undisturbed core samples from each soil depth to measure K_s . Soil samples were saturated from the bottom in a constant-head basin for a minimum of 2 d before testing. The temperature of the water was held constant at $22.5 \pm 1.5^\circ\text{C}$. Multistep outflow tests were also performed. A manual hanging column test was run on one of the undisturbed cores to determine the soil moisture retention curve, $\theta(h)$ (Dane and Hopmans, 2002). The soil sample was placed in a Tempe cell on a 0.1-MPa porous plate and saturated slowly from the bottom with a $0.005 \text{ mol L}^{-1} \text{ CaSO}_4$ and 0.3 g L^{-1} thymol solution for several days (Klute and Dirksen, 1986). Increasingly negative pressure heads (-10 , -20 , -30 , -40 , -50 , -60 , -70 , -80 , -90 , -110 , -130 , and -150 cm of water) were applied by lowering a burette below the Tempe cell. The other sample was tested using a pressure cell; positive pressure was applied incrementally at the top of the soil sample in similar magnitude steps. Previous studies have shown the two methods to produce comparable results (Figueras and Gibb, 2009). At each step, cumulative outflow volume was measured with time until outflow ceased (24–48 h). After 48 h at the final applied pressure step, the wet weights of

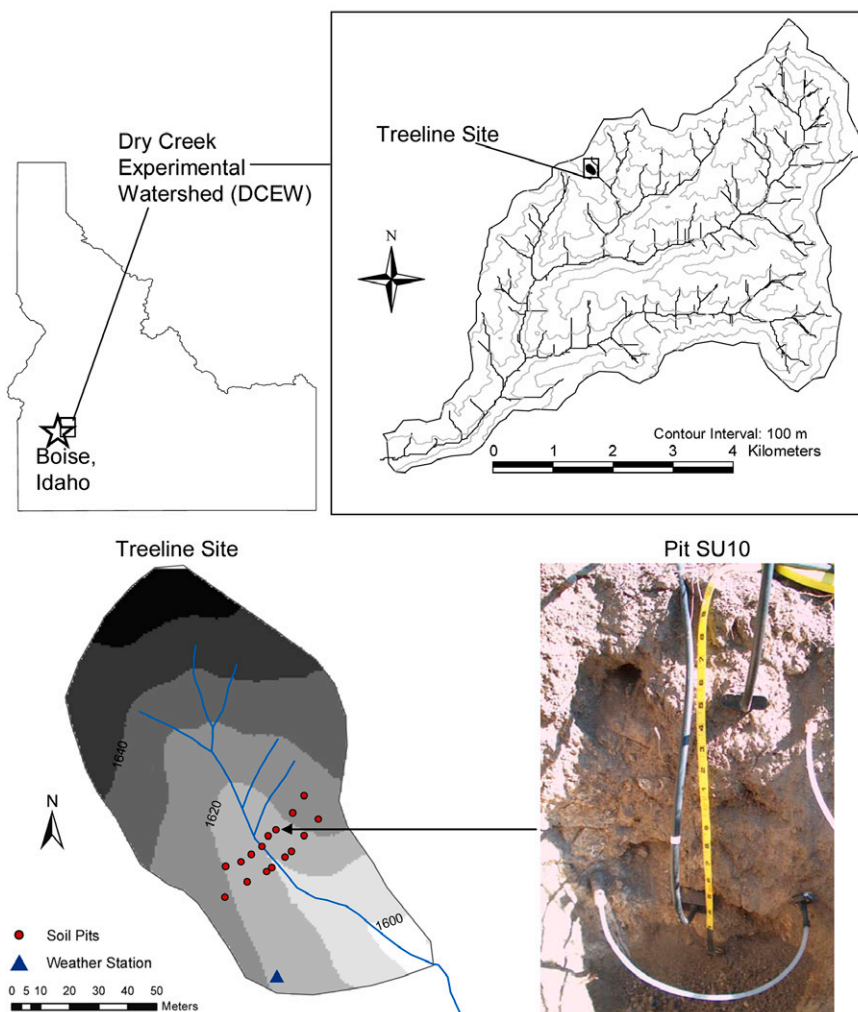


FIG. 1. Location of study site.

the samples were obtained. The samples were subsequently oven dried at 105°C for 24 h to obtain the dry soil weights. Soil moisture contents were back-calculated at each step to obtain points on the $\theta(h)$ curve.

Soil Hydraulic Properties

The van Genuchten (1980) and Mualem (1976) models for the unsaturated soil hydraulic properties were used in this work:

$$\theta(h) = \frac{\theta_s - \theta_r}{\left[1 + (\alpha|h|)^n\right]^m} + \theta_r, \quad h < 0 \quad [1]$$

$$\theta(h) = \theta_s, \quad h = 0$$

$$K(h) = \frac{K_s \left\{1 - (\alpha|h|)^{mn} \left[1 + (\alpha|h|)^n\right]^{-m}\right\}^2}{\left[1 + (\alpha|h|)^n\right]^{ml}}, \quad h < 0 \quad [2]$$

$$K(h) = K_s, \quad h = 0$$

where $\theta(h)$ is the volumetric moisture content at a specific pressure head (h); θ_r and θ_s are the residual and saturated volumetric moisture contents, respectively; α (cm^{-1}), n , and m (where m is typically set equal to $1 - 1/n$) are the van Genuchten fitting parameters; $K(h)$ is the hydraulic conductivity at a specific pressure head; K_s (cm d^{-1}) is the saturated hydraulic conductivity; and l is the pore connectivity parameter that is typically set equal to 0.5 (Mualem, 1976) but can be optimized. Hydraulic parameters for each layer at SU10 were obtained using several techniques: (i) in situ measurements, (ii) laboratory MSO and falling-head tests, (iii) the use of PTFs based on neural networks and multiple linear regression, and (iv) inversion of field data. In addition, we explored three methods for scaling the MSO and PTF measurements or estimates with field information to improve their fits to the in situ data.

Fit of In Situ Data

Time domain reflectometry soil moisture content and tensiometric head data measured in situ were fitted to Eq. [1] with RETC (van Genuchten et al., 1991), a nonlinear least squares fitting computer code. Hydraulic conductivity curves were estimated using Eq. [2] and the van Genuchten (1980) parameters α and n for the in situ data, paired with K_s values obtained from laboratory falling-head tests. The l parameter was set equal to 0.5. The in situ data served as the basis of comparison for all other techniques described below.

Scaled In Situ

Basile et al. (2003) asserted that differences between retention curves measured in the field and in the laboratory are due to differences in imposed boundary conditions. In the case of field application of the instantaneous profile method (Watson, 1966), wetting occurs from the top down, whereas laboratory MSO or evaporation method testing begins with slowly wetting core samples from the bottom. These differences in the mode of water application lead to the generation of different hysteretic branches of the retention curve, with the laboratory drainage curves yielding the highest moisture contents. Basile et al. (2003) proposed combining the estimates of θ_s and the α parameter

(from the results of fitting the moisture content and pressure head readings obtained during the “early” stages of an instantaneous profile method test to Eq. [1]) with the hydraulic parameters obtained via laboratory evaporation experiments (e.g., θ_r and n) to reduce the period during which field measurements are taken. As our laboratory retention curves also showed much higher moisture contents than field measurements for the same pressure heads, we combined the estimates of θ_s and the α parameter from MSO tests with θ_r and n obtained from fitting the in situ moisture content and pressure head data collected under natural precipitation conditions.

Multistep Outflow Tests

The results of MSO tests were also fit with RETC to obtain parameter values for Eq. [1]. Hydraulic conductivity curves were estimated by using Eq. [2] and the van Genuchten (1980) parameters α and n derived from the MSO test with K_s from falling-head tests. Parameter l was again set equal to 0.5.

Pedotransfer Functions

We applied two neural network based PTFs to predict the parameters in Eq. [1] and [2] from soil particle size and bulk density data, and in some cases, organic C content. The first PTF, Rosetta (Schaap et al., 1998, 2001), a public domain code, is based on a wide range of soil types consisting of 2134 soil samples, of which the gravel content is not documented (but probably minimal). This PTF was selected due to its widespread use and availability.

Rosetta requires inputs of percentages of sand (0.05–2 mm), silt (0.002–0.05 mm), and clay (<0.002 mm) and bulk density. Our soil samples had appreciable gravel contents, but since Rosetta does not account for gravel, these percentages were normalized to 100%. The values of θ_s and θ_r predicted by Rosetta were then corrected for the gravel dead volume, which was assumed not to participate in the water storage capacity of the soil (Bouwer and Rice, 1983):

$$\theta_b = (1 - V_g) \theta_r \quad [3]$$

where θ_b is the volumetric moisture content of the gravel–soil mixture ($\text{m}^3 \text{m}^{-3}$), V_g is the volume fraction of the gravel ($\text{m}^3 \text{m}^{-3}$), and θ_r is the volumetric moisture content of the soil minus the gravel ($\text{m}^3 \text{m}^{-3}$).

The second neural network based PTF used was previously developed for coarse-textured soils, similar to those at the Dry Creek Experimental Watershed. This PTF, called the Hanford PTF here, was created for soils of the Hanford Formation (Hanford, WA) (Ye et al., 2007; Schaap et al., 2003). Gravel percentages of this data set ranged between 0 and 18%, with an average of 1.5% (Schaap, personal communication, 2007).

Two multiple linear regression based PTFs were also applied, based on their successful use in other studies (e.g., Chanzy et al., 2008). The Rawls and Brakensiek (1985) PTF (RB) was created using the Soil Conservation Service database, which contains data from thousands of U.S. agricultural soils and is applicable for soils with sand percentages between 5 and 70%, and clay between 5 and 60%. The Wösten et al. (1999) model (WOE) was based on soils data from several European countries. Although the minimum and maximum percentages of the sand and clay particle sizes were not specifically stated, the soil data used in

the PTF ranged from coarse to very fine materials. The Wösten model accounts for particle size, bulk density, and organic C content. As only the Hanford PTF accounts for gravel content, the percentages of sand, silt, and clay were normalized to neglect the gravel content of the samples, and Eq. [3] was used to correct the moisture contents accordingly for the Rosetta, RB, and WOE PTFs.

Scaling

Given the less-than-optimal fit of the in situ data by the MSO and PTF curves (see below), we attempted to improve these fits and ultimately the predictions of soil moisture contents with time by “scaling” the predicted moisture retention curves described above to the range of moisture contents actually observed in the field. To do this, we tried two approaches in addition to the Basile scaling method discussed above. First, we replaced the predicted values of θ_s and θ_r for all of the above $\theta(h)$ curves with the maximum and minimum moisture contents measured at the sensor locations of interest. These are referred to hereafter as the S1 curves, or field-scaled estimates (e.g., Rosetta_{S1} and so on). Second, we set θ_s equal to the field-measured value as before, but calculated the appropriate θ_r by solving Eq. [1] for θ_r for a known point on the in situ retention curve at the dry end of the range of measured values (for SU10, the lowest reliable measurement for pressure head was approximately -300 cm). We refer to these as the S2 curves (Rosetta_{S2}, etc.). Thomasson et al. (2006) applied a similar approach to scale unsaturated hydraulic conductivity curves measured on soil cores in the laboratory by using a single field measurement of unsaturated hydraulic conductivity at a known moisture content to replace K_s as the matching point.

The accuracy of the various soil moisture retention curves compared with the in situ measurements was assessed by calculating the RMSE:

$$\text{RMSE}_{\theta(h)} = \sqrt{\frac{1}{K} \sum_{i=1}^K [\theta(h)_i - \hat{\theta}(h)_i]^2} \quad [4]$$

where $\theta(h)_i$ and $\hat{\theta}(h)_i$ are the measured and predicted volumetric moisture contents for $K = 31$ points along the moisture retention curve from $h = 0$ to $h = -300$ cm.

Soil Moisture Modeling

To compare the effects of different soil hydraulic property inputs, we simulated the one-dimensional soil moisture dynamics in SU10 from 27 Feb. to 6 May 2003 (Days of the Year [DOY] 58–126) when the soil was in a wet state, after the primary snowmelt event and before the spring dry-down period (Fig. 2). The primary snowmelt event occurred in January, after which the catchment received intermittent rain and snow for the remainder of the winter.

We used HYDRUS-1D, a public domain, unsaturated–saturated flow and inversion code for one-dimensional problems (Šimůnek et al., 2005; available at www.pc-progress.cz/Fr_Hydrus1D.htm [verified 21 Dec. 2008]). The model solves the Richards (1931) equation for one-dimensional vertical water flow:

$$\frac{\partial}{\partial z} \left[K(h) \left(\frac{\partial h}{\partial z} + 1 \right) \right] - S = \frac{\partial \theta}{\partial t} \quad [5]$$

where $K(h)$ is the unsaturated hydraulic conductivity (cm s^{-1}) as a function of h (cm); θ is the volumetric moisture content ($\text{m}^3 \text{m}^{-3}$) as a function of pressure head; z is the spatial coordinate (cm) positive upward; and S ($\text{m}^3 \text{m}^{-3} \text{s}^{-1}$) represents the root water extraction rate, defined by Feddes et al. (1978) as

$$S(h, z) = \alpha(h) S_{\max}(h, z) \quad [6]$$

where α is a dimensionless water stress reduction factor as a function of pressure head h (cm) (unrelated to the α parameter of Eq. [1]), S_{\max} ($\text{m}^3 \text{m}^{-3} \text{s}^{-1}$) is the maximum possible root water extraction rate when soil water is not limiting, and z is the soil depth (cm). No detailed measurements of the vegetation parameters, except maximum rooting depth (Williams, 2005), were conducted on the vegetation at the Treeline site, so the S-shaped water stress response function (van Genuchten, 1987) was used:

$$\alpha(h) = \frac{1}{1 + (h/h_{50})^{p_1}} \quad [7]$$

where h_{50} is the pressure head at which root water uptake is reduced by 50% and p_1 is an adjustable parameter. In our study, the values of $p_1 = 3$ and $h_{50} = -3000$ cm were used. The h_{50} value

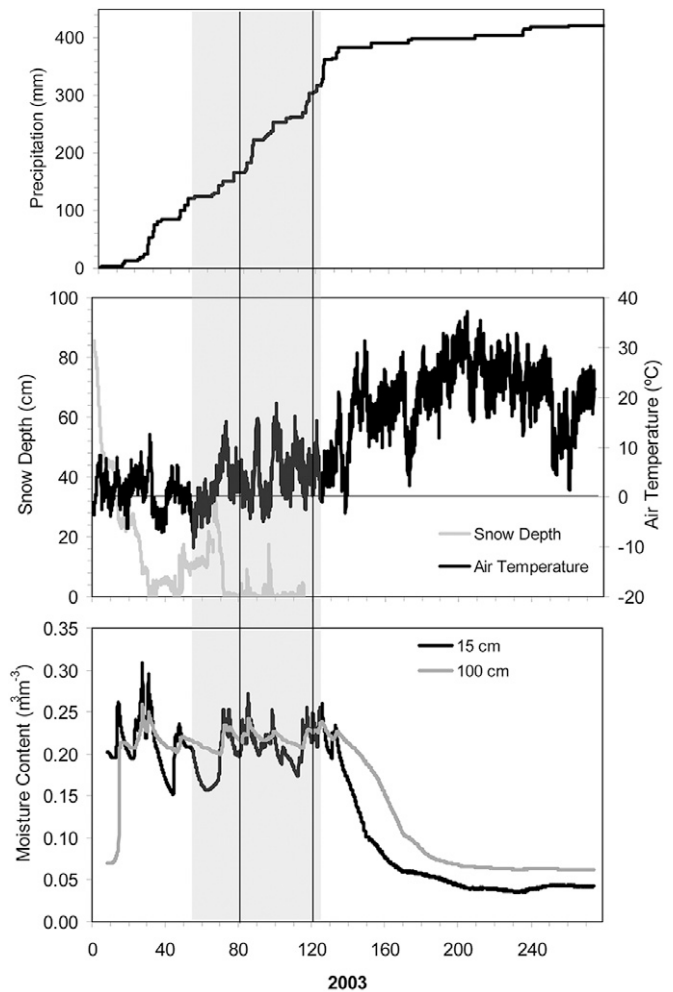


FIG. 2. Hydrometeorologic conditions during the study period. The vertical gray section indicates the extended simulation period. The vertical black lines indicate the start date of precipitation events used for inversion. The soil moisture values are from a pit on the northeast-facing slope near the weather station.

was set equal to a value used for grass in another arid region study (Guan, 2005).

The air phase was assumed to play an insignificant role in the liquid flow process, and water flow due to thermal gradients was neglected. Following the work of Vogel et al. (2000), we used Eq. [2] with a small non-zero air-entry value of -2 cm. The use of a small air-entry pressure head has little effect on the character of the soil moisture retention curve, but provides better numerical stability for small values of n .

The soil profile at SU10 was discretized in 0.5-cm increments from the soil surface to the location of the lower tensiometer (52 cm below the ground surface). The soil profile was modeled as a two-layer system with differing soil hydraulic properties (0–24 and 24–52 cm). This modeling domain was then used for subsequent direct and inverse simulations with the different soil hydraulic property estimates described above.

An atmospheric boundary condition was imposed on the soil surface to account for precipitation and evapotranspiration. This boundary condition in HYDRUS-1D does not account for surface runoff, which was not observed at the site during the periods of interest. Since HYDRUS-1D does not include a snowmelt component, we used the Simultaneous Heat and Water (SHAW) model (Flerchinger et al., 1996) to capture the appropriate timing of soil water input from mixed-phase precipitation and create the input file for HYDRUS-1D. The SHAW model determines if the precipitation is rain or snow depending on air temperature and simulates the melt of accumulated snow using an energy balance approach. Except for the snowmelt event in early March 2003, precipitation was predominantly rain with occasional minor snow events (Fig. 2). The bottom boundary was set equal to the measured pressure heads at the lower tensiometer and the initial conditions for each layer were assigned to the moisture contents measured by the TDR probes.

Effective hydraulic parameters for SU10 were obtained by inversion by minimizing an objective function, Φ , that expressed the differences between modeled and measured moisture at the sensor locations (15 and 52 cm) and the pressure head at the upper sensor location during two short spring precipitation events in 2003, 24–31 March and 2–6 May (DOY 83–90 and 122–126, respectively; Fig. 2). These periods were selected because they followed snowmelt and subsequent tensiometer de-airing, and ran from the beginning of precipitation to the time when the soil moisture content returned to initial conditions. In both events, precipitation occurred as a mixture of rain and snow. The objective function was defined as (Šimůnek et al., 2005)

$$\Phi(\mathbf{b}, q, p) = \sum_{j=1}^m v_j \sum_{i=1}^{n_j} [q_j^*(z, t_i) - q_j(z, t_i, \mathbf{b})]^2 \quad [8]$$

where the right-hand side represents deviations between the measured (q_j^*) and calculated (q_j) moisture contents at the two measurement depths and the pressure head at the upper sensor location; m is the number of different sets of measurements; n_j is the number of measurements in a particular measurement set; $q_j^*(z, t_i)$ represents a specific measurement at time t_i for the j th measurement set at depth z ; $q_j(z, t_i, \mathbf{b})$ are the corresponding model predictions for the vector of estimated parameters \mathbf{b} (θ_s, α, n, K_s); and the weighting factor, v_j , is

given by the inverse of the number of measurements multiplied by the variance of those observations (Clausnitzer and Hopmans, 1995). The parameters l and θ_r were not optimized to simplify the inversion process.

To achieve stable estimates, parameters were optimized in a sequential fashion as suggested by Šimůnek and van Genuchten (1996). The estimated parameters obtained from the inversion of Event 1 (DOY 83–91) data were used as initial estimates for the inversion of Event 2 (DOY 122–126) data. We then used the estimated parameters from the inversion of Event 2 data as initial estimates, and inverted the Event 1 data once more to obtain the final effective soil hydraulic parameters for the SU10 profile. These parameter sets were then used to predict the soil moisture at the two sensor locations and the pressure head at the shallow sensor location for an extended period (27 Feb.–6 May 2003).

The goodness of fit of the various simulations was quantified using the RMSE values (Eq. [9]) calculated based on the predicted vs. measured moisture contents at both sensor locations for the entire simulation period. Systematic errors between measurements and predictions were evaluated with mean residual (MR) values (Eq. [10]):

$$\text{RMSE}_{\theta(t)} = \sqrt{\frac{1}{L} \sum_{i=1}^L [\theta(t)_i - \hat{\theta}(t)_i]^2} \quad [9]$$

$$\text{MR}_{\theta(t)} = \frac{1}{L} \sum_{i=1}^L [\theta(t)_i - \hat{\theta}(t)_i] \quad [10]$$

where L is the number of estimated and measured values, and $\theta(t)_i$ and $\hat{\theta}(t)_i$ are the measured and predicted volumetric moisture contents at both depths for hourly time steps during the extended simulation period. Mass balance errors for simulations were also computed.

As one of the measures of accuracy of soil hydraulic parameters estimates, we also evaluated the predicted cumulative soil water flux at the bottom of the profile for the different sets of hydraulic parameter inputs.

Results

Physical Properties

The physical properties of the soil samples with depth at SU10 are presented in Table 1. All soil samples were classified as gravelly sands according to the USDA textural classification system (Soil Survey Staff, 1975). Among the tested samples, gravel content ranged from 15 to 27% in the shallow (0–24 cm) and 13 to 38% in the deep (24–52 cm) soil layers and the combined silt and clay fraction ranged in value from 1 to 13%.

TABLE 1. Soil properties at Pit SU10.

Soil layer	Core depth	Bulk density	Particle density	Gravel	Coarse sand	Fine sand	Silt and Clay	
							Silt	Clay
	cm	g/cm ³		%				
0–24	12–18	1.22	—	22.3	59.2	17.5	1.0	0
	20	1.54	2.58	15.1	55.4	16.9	9.6	2.9
	20	1.63	2.61	27.3	51.6	13.2	5.3	2.6
24–52	46–52	1.28	—	38.1	50.5	10.3	1.0	0
	40	1.62	2.54	12.8	54.8	22.4	8.1	2.0
	40	1.60	2.56	24.7	55.3	15	5.0	

Retention Curves

Soil moisture retention curves for each layer were estimated from inversion of the field data with Eq. [8], MSO data, the Basile et al. (2003) scaling approach, and the two additional scaling approaches described above: S1, in which the field-measured maximum and minimum θ values were used to replace θ_s and θ_r , and S2, in which the field-measured maximum θ value was used

to replace θ_s and θ_r was calculated by fixing a point at the dry end of the in situ retention curve (Fig. 3 and 4). The soil hydraulic parameters are listed in Table 2, and the RMSE values (Eq. [4]) describing the fits of the inversely estimated, laboratory-measured, or PTF-predicted curves to the in situ retention data are shown in Table 3. The $\theta(h)$ curves obtained from the various methods show

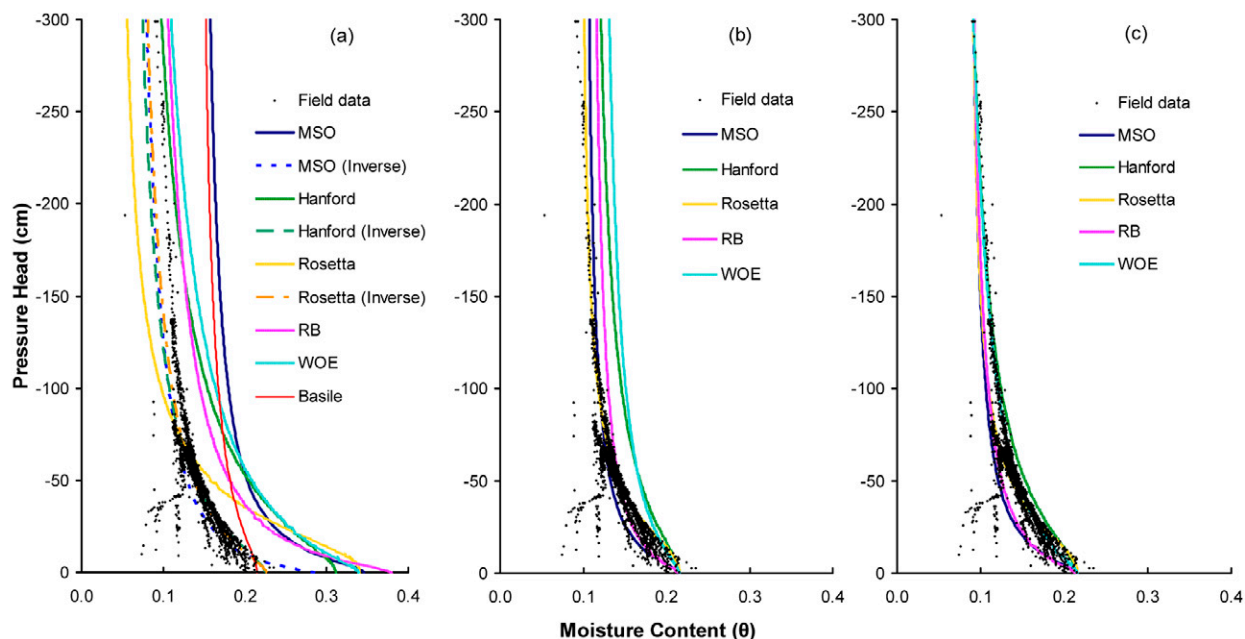


FIG. 3. Moisture content as a function of pressure head for the shallow soil layer (0–24 cm) at Pit SU10 as determined by several estimation and measurement techniques: (a) curves from Rosetta, Rawls and Brakensiek (RB), Wösten (WOE), and Hanford pedotransfer functions, multistep outflow (MSO), Basile scaling, and inversion of field data obtained with initial estimates from these sources vs. in situ data; (b) saturated (θ_s) and residual (θ_r) volumetric moisture contents replaced by field-measured values (S1 scaling approach); and (c) θ_s replaced by field-measured values and θ_r calculated by fitting a point on the retention curve near -300 cm (S2 scaling approach).

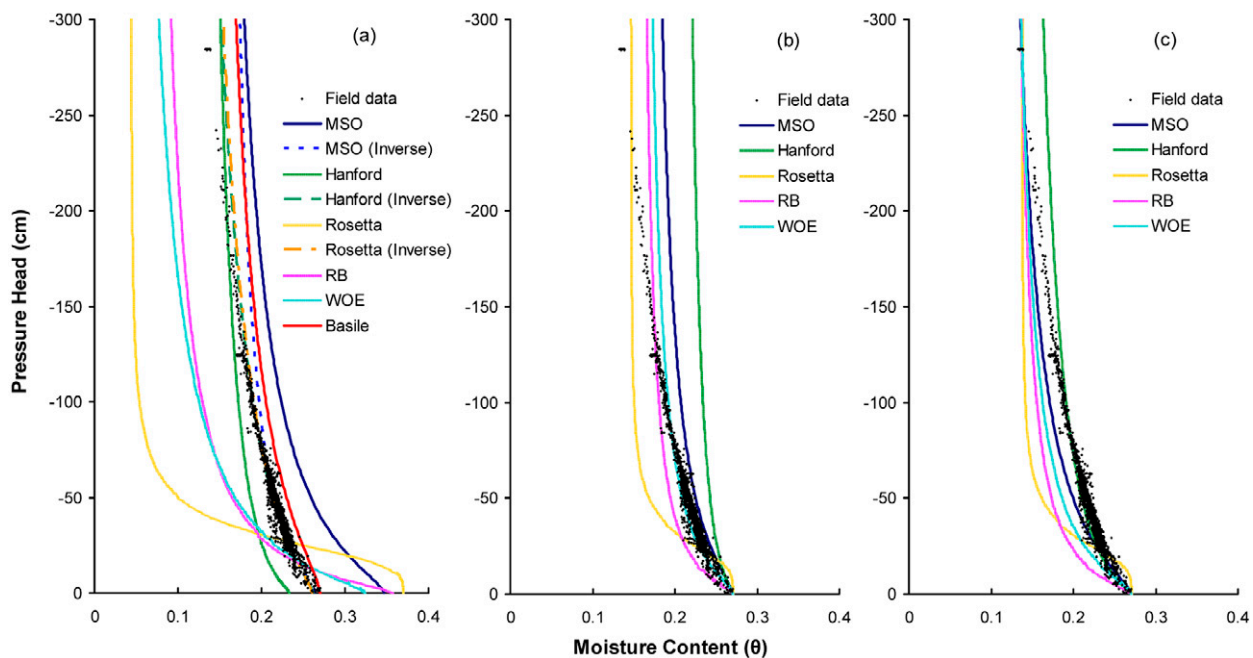


FIG. 4. Moisture content as a function of pressure head for the deep soil layer (24–52 cm) at Pit SU10 as determined by several estimation and measurement techniques: (a) curves from Rosetta, Rawls and Brakensiek (RB), Wösten (WOE), and Hanford pedotransfer functions, multistep outflow (MSO), Basile scaling, and inversion of field data obtained with initial estimates from these sources vs. in situ data; (b) saturated (θ_s) and residual (θ_r) volumetric moisture contents replaced by field-measured values (S1 scaling approach); and (c) θ_s replaced by field-measured values and θ_r calculated by fitting a point on the retention curve near -300 cm (S2 scaling approach).

significant variability, as observed in other studies (Mallants et al., 1997; Gribb et al., 2004; Green et al., 2005; Chanzy et al., 2008). As expected, the $\theta(h)$ curves obtained from inversion yielded the best RMSE $_{\theta(h)}$ values (0.003–0.020 m³ m⁻³) for fit to the in situ retention data (Table 3, Fig. 3a and 4a) for both layers. It is important to note, however, that we were able to successfully invert the field data because we had information about bottom boundary conditions as well as measured moisture content and pressure heads in both layers. A lack of knowledge of the bottom boundary conditions would yield inversely estimated parameters that would depend on the assumed boundary conditions.

For the shallow layer, the MSO $\theta(h)$ curve has a similar appearance to the in situ data, but θ values are consistently higher than those measured in the field (Fig. 3a), with RMSE $_{\theta(h)} = 0.068$ m³ m⁻³, consistent with the observations of Green et al. (2005) and Basile et al. (2003), who also found that laboratory-derived curves overestimated the moisture content for a given pressure head when compared with field measurements. The Basile approach yielded a similar curve (RMSE $_{\theta(h)} = 0.049$ m³ m⁻³). The $\theta(h)$ curves predicted by the Hanford, WOE, and RB PTFs are similar to each other, consistently overestimating the moisture content of the soil, but to a lesser degree as the pressure head decreased toward -300 cm (RMSE $_{\theta(h)} = 0.044$ – 0.052 m³ m⁻³). Rosetta also initially overestimated the moisture content from saturation to approximately -70 cm, and then underestimated $\theta(h)$ values for lower pressure heads [RMSE $_{\theta(h)} = 0.05$ m³ m⁻³].

When the θ_s and θ_r values were scaled to the maximum and minimum measured moisture contents as described above (scaling approach S1; Table 3 and Fig. 3b), all of the fits of the curves to the in situ data in the shallow layer were much improved; the Rosetta_{S1} and MSO_{S1} curves are the best, with RMSE $_{\theta(h)}$ values of 0.006 and 0.01 m³ m⁻³ (Table 3). The fit of the Hanford, RB, and WOE curves were further improved using the second scaling approach (S2; Fig. 3c) with RMSE $_{\theta(h)}$ values ranging from 0.003 to 0.011 m³ m⁻³ (Table 3).

In the deep layer (24–52 cm below the ground surface), as with the shallow layer, the MSO curve has a similar curvature as the in situ curve, but with elevated moisture contents for given pressure head values [RMSE $_{\theta(h)} = 0.039$ m³ m⁻³]. The Basile curve lies between the MSO and in situ curves [RMSE $_{\theta(h)} = 0.016$ m³ m⁻³]. The $\theta(h)$ curves predicted by the Rosetta, WOE, and RB PTFs yielded even poorer representations of the in situ $\theta(h)$ curve than they did for the shallow layer [RMSE $_{\theta(h)} = 0.059$ – 0.117 m³ m⁻³] (Table 3, Fig. 4a). These PTFs significantly

TABLE 2. The van Genuchten (1980) hydraulic parameters residual and saturated volumetric moisture content (θ_r and θ_s , respectively), shape-fitting parameters (α and n), pore connectivity parameter (l), and saturated hydraulic conductivity (K_s) for Pit SU10 obtained from various measurement and estimation techniques, including inversion.

Source of hydraulic parameters	Depth	θ_r	θ_s	α	n	l	K_s
	cm	— m ³ m ⁻³ —	— m ³ m ⁻³ —	cm ⁻¹			cm d ⁻¹
In situ data	0–24	0.07	0.20	0.040	1.70	0.50	692†
	24–52	0.06	0.27	0.026	1.40	0.50	320†
Multistep outflow	0–24	0.14	0.35	0.121	1.62	0.50	692†
	24–52	0.10	0.35	0.046	1.44	0.50	320†
Rosetta	0–24	0.04	0.34	0.040	2.17	-0.85	196
	24–52	0.04	0.37	0.038	3.59	-0.81	1390
Basile et al. (2003)	0–24	0.14	0.22	0.040	1.62	0.50	692†
	24–52	0.10	0.27	0.026	1.44	0.50	320†
Hanford	0–24	0.04	0.31	0.036	1.63	0.50	160
	24–52	0.02	0.23	0.095	1.15	0.50	66
Rawls and Brakensiek (1985)	0–24	0.05	0.38	0.138	1.47	0.50	18
	24–52	0.04	0.36	0.121	1.52	0.50	15
Wösten et al. (1999)	0–24	0.01	0.34	0.060	1.41	-1.00	81
	24–52	0.01	0.32	0.072	1.50	-0.13	43
Inverse solution	0–24	0.07‡	0.27	0.131	1.57	0.50‡	45
	24–52	0.06‡	0.26	0.030	1.38	0.50‡	156

† K_s value obtained from falling head permeability testing of undisturbed samples.

‡ Not optimized.

overestimated the maximum moisture contents and then greatly underestimated the lowest measured moisture contents; the curves do not follow the in situ data at all. On the other hand, the Hanford PTF fits much better. It initially underestimated the saturated moisture content, but it yielded a curve that is similar to the in situ data and that improved as the pressure head decreased [RMSE $_{\theta(h)} = 0.02$ m³ m⁻³] (Fig. 4a).

In summary, only the Hanford PTF and Basile curves provided reasonable approximations of the in situ behavior (Fig. 4a). Replacing θ_s and θ_r with field-measured values (S1 scaling) again improved the fits of all curves except the Hanford_{S1} curve, but not to the extent seen for the shallower depth (RMSE values ranged from 0.014– 0.028 m³ m⁻³ for WOE_{S1}, RB_{S1}, MSO_{S1}, and Rosetta_{S1}; Table 3, Fig. 4b). When the hydraulic parameters were

TABLE 3. Root mean square errors for retention curves measured in the laboratory and predicted by pedotransfer functions compared with in situ curves. S1 and S2 refer to the scaled parameters: S1 parameters were obtained by replacing the saturated (θ_s) and residual (θ_r) moisture contents with the maximum and minimum field-measured moisture contents; S2 was obtained by setting θ_s equal to the maximum field-measured value and calculating θ_r by solving Eq. [1] for θ_r for a known point at the dry end of the field-measured moisture contents. Inverse refers to parameters obtained from inversion of field data obtained with initial estimates from these sources.

Source of hydraulic parameters	Depth	RMSE			
		Unscaled	S1	S2	Inverse
	cm	m ³ m ⁻³			
Multistep outflow	0–24	0.068	0.010	0.012	0.016
	24–52	0.039	0.024	0.016	0.003
Rosetta	0–24	0.050	0.006	0.008	0.010
	24–52	0.117	0.028	0.035	0.004
Basile et al. (2003)	0–24	0.049	—	—	0.011
	24–52	0.016	—	—	0.012
Hanford	0–24	0.044	0.026	0.007	0.015
	24–52	0.020	0.052	0.009	0.003
Rawls and Brakensiek (1985)	0–24	0.045	0.015	0.011	0.020
	24–52	0.059	0.015	0.030	0.016
Wösten et al. (1999)	0–24	0.052	0.032	0.003	0.018
	24–52	0.065	0.014	0.023	0.012

adjusted using the second scaling approach (S2), the $RMSE_{\theta(t)}$ values decreased only for the Hanford_{S2} and MSO_{S2} curves (0.009 and 0.016 $m^3 m^{-3}$, respectively) compared with using the first approach (S1) but increased in the other cases (but not as high as the unscaled values; Table 3, Fig. 4c).

Forward Simulations with Different Soil Hydraulic Property Inputs

Figures 5a to 5c show representative results from simulating infiltration at SU10 from 27 Feb. to 6 May 2003 (DOY 58–126) for the MSO, WOE, and Hanford PTF inputs (results for Rosetta, RB, and Basile inputs not shown). In all cases, the mass balance errors were $<0.001\%$. First, we present the results obtained using the hydraulic parameters obtained from inversion, Basile scaling, and the various PTFs and MSO tests, followed by the results obtained with the scaling inputs, S1 and S2.

The hydraulic parameters obtained from inversion of two short precipitation events yielded the best fit of the $\theta(t)$ data during the extended simulation period with $RMSE_{\theta(t)}$ (Eq. [9]) values ranging from 0.008 to 0.010 $m^3 m^{-3}$ and $MR_{\theta(t)}$ (Eq. [10]) values of -0.002 to $0.004 m^3 m^{-3}$ (Table 4, simulation results not shown). These parameter inputs for the profile resulted in a lower RMSE value than the use of the hydraulic parameters derived

from the in situ data [$RMSE_{\theta(t)} = 0.020 m^3 m^{-3}$] (simulation results not shown).

The Basile scaled parameters yielded a lower $RMSE_{\theta(t)}$ value (0.030 $m^3 m^{-3}$) than any of the unscaled PTFs or the unscaled MSO inputs. In this case, $\theta(t)$ values were overestimated for both layers during the entire simulation period (simulation results not shown), as indicated by a $MR_{\theta(t)}$ value of $-0.024 m^3 m^{-3}$.

The next best fit of the $\theta(t)$ data was obtained with the Hanford PTF parameter estimates [$RMSE_{\theta(t)} = 0.034 m^3 m^{-3}$, $MR_{\theta(t)} = -0.002 m^3 m^{-3}$; Table 4, Fig. 5a]. The use of WOE parameters [$RMSE_{\theta(t)} = 0.042 m^3 m^{-3}$, $MR_{\theta(t)} = -0.005 m^3 m^{-3}$] led to continuous overestimation of moisture content in the shallow layer and underestimation in the deep layer (except for DOY 70, 85, 117, and 125 when the moisture content was overestimated by 3–6%; Table 4, Fig. 5b). When the MSO parameters were used as inputs (Fig. 5c), moisture contents were consistently overestimated in both shallow and deep layers [$RMSE_{\theta(t)} = 0.055 m^3 m^{-3}$, $MR_{\theta(t)} = -0.053 m^3 m^{-3}$]. This significant overestimation of $\theta(t)$ for both depths is due to the fact that the $\theta(h)$ curves at both depths were shifted toward higher moisture contents than the field curves (Fig. 3a and 4a), as discussed above. The RB and Rosetta parameters yielded the worst fits, with $RMSE_{\theta(t)}$ values of 0.057 and 0.068 $m^3 m^{-3}$, respectively (results not shown). Use of the RB parameters resulted in moisture responses that were too

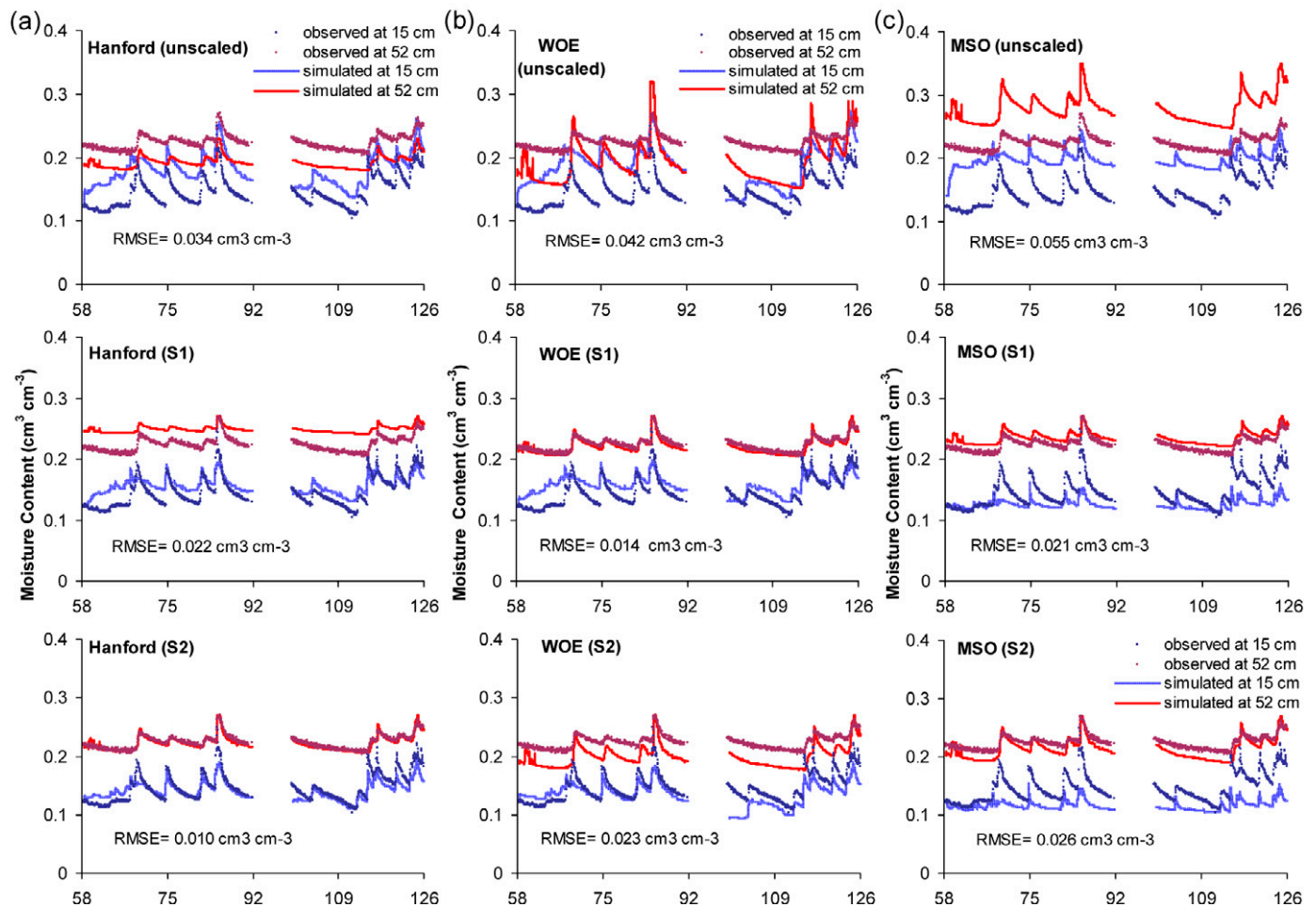


FIG. 5. Field-measured moisture contents at two depths and results of direct simulations for Days of the Year (DOY) 58 to 126, 2003. Soil hydraulic parameter inputs obtained from (a) the Hanford pedotransfer function (PTF), (b) the Wösten PTF, and (c) multistep outflow test data using saturated hydraulic conductivity values from falling-head tests. Missing data for DOY 90 to 100 were due to equipment malfunction.

TABLE 4. Root mean square errors and mean residuals (MR) for simulated soil moisture contents over time for each of the scaled and unscaled hydraulic parameter sets over the extended simulation period, and cumulative water flux across the bottom of the simulated soil profile ($z = 52$ cm). S1 and S2 refer to the scaled parameters: S1 parameters were obtained by replacing the saturated (θ_s) and residual (θ_r) water contents with the maximum and minimum field-measured moisture contents; S2 was obtained by setting θ_s equal to the maximum field-measured value and calculating θ_r by solving Eq. [1] for θ_r for a known point at the dry end of the field-measured moisture contents. Inverse refers to parameters obtained from inversion of field data obtained with initial estimates from these sources.

Source of hydraulic parameters	RMSE				MR†				Fluxes‡			
	Unscaled	S1	S2	Inverse	Unscaled	S1	S2	Inverse	Unscaled	S1	S2	Inverse
	$\text{m}^3 \text{m}^{-3}$								cm			
In situ	0.02	–	–	0.008	0.004	–	–	0.001	-8.4	–	–	-13.6
Multistep outflow	0.055	0.021	0.026	0.009	-0.053	0.004	0.02	0.002	-8.4	-11.1	-11.7	-12.7
Rosetta	0.068	0.031	0.037	0.01	0.04	0.024	0.03	0.002	-8.5	-9.1	-9.4	-10.7
Basile et al. (2003)	0.030§	–	–	0.009	-0.024	–	–	0.002	-7.6	–	–	-12.8
Hanford pedotransfer function	0.034	0.022	0.01	0.01	-0.002	-0.018	0.003	0.004	-7.9	-7.5	-8.4	-12.3
Rawls and Brakensiek (1985)	0.057	0.016	0.029	0.01	-0.015	0.005	0.02	-0.002	-8.7	-14	-14.1	-12.9
Wösten et al. (1999)	0.042	0.014	0.023	0.01	-0.005	-0.005	0.017	0.004	-6.9	-8.4	-9.1	-11.8

† Underestimation or overestimation.

‡ Inflow and outflow.

§ Basile scaling approach where saturated volumetric water content θ_s and fitting parameter α are obtained from the field data and residual volumetric water content θ_r and fitting parameter n are from the multistep outflow test results.

high in the shallow layer and too low in the deep layer, except for 4 d when the moisture content was overestimated. An MR value of $-0.015 \text{ m}^3 \text{ m}^{-3}$ indicates an overall overestimation of moisture content in both layers. The use of Rosetta parameters led to significant underestimation of $\theta(t)$ in the deep layer, with overly dynamic responses to precipitation that resulted in overestimations of >12% on 4 d and a slight underestimation of the $\theta(t)$ in the shallow layer. An $\text{MR}_{\theta(t)}$ value of $0.040 \text{ m}^3 \text{ m}^{-3}$ reflects this systematic underestimation of moisture content.

Scaling the moisture content inputs by the minimum and maximum field-measured values (Fig. 3b and 4b) improved the $\text{RMSE}_{\theta(t)}$ values for the simulations of $\theta(t)$ in all cases (Table 4). The $\text{RMSE}_{\theta(t)}$ values decreased most significantly with the S1 approach for Rosetta_{S1} ($0.031 \text{ m}^3 \text{ m}^{-3}$), MSO_{S1} ($0.021 \text{ m}^3 \text{ m}^{-3}$), and the RB_{S1} PTF ($0.016 \text{ m}^3 \text{ m}^{-3}$). The MR values significantly improved for all estimates (-0.005 to $0.024 \text{ m}^3 \text{ m}^{-3}$), except for the Hanford_{S1} PTF, for which the overestimation of moisture content increased compared with the unscaled approach (MR = -0.018 vs. $-0.002 \text{ m}^3 \text{ m}^{-3}$; Table 4).

When using the S2 approach, the $\text{RMSE}_{\theta(t)}$ value decreased compared with the S1 value only for the Hanford_{S2} PTF (0.010 vs. $0.022 \text{ m}^3 \text{ m}^{-3}$; Table 4). In all other cases (Rosetta_{S2}, MSO_{S2}, RB_{S2}, and WOE_{S2}), the $\text{RMSE}_{\theta(t)}$ values were greater than for S1, but not as large as the $\text{RMSE}_{\theta(t)}$ values for the unscaled values. The S2 approach yielded an underestimation of moisture content in all cases, with the Hanford_{S2} PTF estimates yielding the lowest value (MR = $0.003 \text{ m}^3 \text{ m}^{-3}$) and the Rosetta_{S2} estimates yielding the highest value (MR = $0.030 \text{ m}^3 \text{ m}^{-3}$).

Interestingly, the simulated cumulative water flux leaving at the bottom of the soil profile did not vary significantly when different sets of unscaled hydraulic parameter values were used as inputs. The cumulative flux of water out of the bottom of the domain obtained with the unscaled MSO, Rosetta, RB, and in situ soil hydraulic parameter inputs ranged from -8.4 to -8.7 cm (Table 4) for the extended simulation period. Fluxes estimated with the use of Basile scaling and Hanford PTF inputs were smaller compared with the other four approaches (-7.6 and -7.9 cm), while the smallest fluxes across the bottom of the profile were obtained with the unscaled WOE PTF inputs (-6.9 cm).

The cumulative outflow increased when the S1 inputs were used (-7.5 to -14.0) except for the Hanford_{S1} parameters; in that case, the flux slightly decreased compared with the value obtained with the unscaled inputs (-7.5 vs. -7.9 cm). With the S2 approach, the cumulative water outflow from the profile increased further for all sets of hydraulic parameter inputs (-8.4 to -14.1 cm).

Simulations performed with the inversely estimated parameters led to higher cumulative water fluxes (-10.7 to -13.6 cm) than those obtained with the other unscaled and scaled inputs, except for the fluxes obtained with the RB_{S1} and RB_{S2} parameters (-14.0 and -14.1 cm, respectively; Table 4).

Discussion

As one might expect, the parameter estimates that yielded the best fits of the in situ $\theta(h)$ data also yielded the best simulations of the $\theta(t)$ data with time. The unscaled MSO inputs consistently overestimated $\theta(h)$, as observed by others. The fits of the various PTFs to the in situ $\theta(h)$ curves were variable and not consistent between the shallow and deep sensor locations. For example, the Hanford PTF overestimated $\theta(h)$ values at the shallow depth, where it is similar in its ability to fit the data compared with the RB and WOE PTFs, but provided the best fit of the data at the deeper location, where the RB and WOE PTFs did not perform as well. The Rosetta PTF performed poorly at both depths. The Basile scaling approach yielded a relatively poor fit of the data in the shallow layer but gave the best fit of the near-saturated $\theta(h)$ values at the deeper sensor location. In all cases except for the Hanford PTF at the deep location, significant improvements in the fit of the estimated $\theta(h)$ curves to the in situ measured $\theta(h)$ curves were obtained by field scaling the predicted or laboratory-measured saturated and residual moisture contents by the maximum and minimum field-measured θ values, although the improvement was more significant for the shallow layer. The second scaling approach, in which the residual moisture contents are estimated by fitting the retention curve through a point of low moisture content on the retention curve, yielded mixed results in terms of improving the fit of the in situ measured $\theta(h)$ curves and only improved the simulation $\text{RSME}_{\theta(t)}$ for the Hanford PTF hydraulic parameter inputs.

We found that accounting for the gravel dead volume with Eq. [3] did not significantly improve the PTF estimates of θ_s and θ_r over the uncorrected values. The gravel content of the soil had an appreciable effect on the character of the $\theta(h)$ curve that cannot be accounted for simply by ignoring it or by applying a simple correction factor. The fact that the Basile scaling approach improved the fit of the MSO curve parameters to the in situ data suggests that the differences in applied boundary conditions between the field and laboratory methods did have a significant effect on the retention curves at our study site. These limited results also suggest that the Basile scaling approach, originally applied to instantaneous profile method test data and laboratory evaporation-derived retention curves, can be successfully extended to in situ measurements of moisture content and pressure head obtained under natural conditions and parameters obtained from MSO data.

The simulation results provide insight into the level of sophistication needed in the hydraulic property inputs to successfully predict soil moisture at two locations in the profile. The soil hydraulic parameters for the profile obtained from inversion of two short rain events in 2003 (24–31 March and 2–6 May, DOY 83–90 and 122–126, respectively) yielded the best predictions of $\theta(z)$ during an extended period (DOY 58–126), but such inversion requires knowledge of the bottom boundary conditions, which are not typically known. Predictions of the retention curves, and consequently the soil moisture predictions using the unscaled RB, WOE, and Rosetta PTFs, were poor; and even though the Hanford PTF performed better, it was not by an appreciable amount. The hydraulic parameter values obtained from laboratory MSO tests yielded no better predictions of soil moisture with time.

We found that simulations of $\theta(z)$ could be significantly improved by simply replacing the saturated and residual moisture contents with the maximum and minimum measured moisture contents, whether the parameters were estimated from PTFs or obtained from MSO measurements. The second scaling approach only improved simulation results when applied to the Hanford PTF.

Water fluxes at the bottom of the soil profile can provide a measure of the potential groundwater recharge, an important quantity in water resources assessment. The simulated cumulative water flux at the bottom of the soil profile generally increased from unscaled to inversely estimated parameter inputs (with the exception of the RB inputs) (Table 4). Although the RMSE values for simulation results with the unscaled, in situ parameters show a good fit of simulated vs. observed soil moisture ($0.020 \text{ m}^3 \text{ m}^{-3}$), the water flux was underestimated by approximately 38% compared with values obtained using the inversely estimated soil hydraulic parameters that were obtained with initial parameters derived from in situ measurements. The simulated water fluxes increased by using the scaled retention curves (S1 and S2) but were still 36 and 31% lower, respectively, than the fluxes obtained with inversely estimated parameters. Thus, in spite of the good fit of simulated vs. observed soil moisture with the use of unscaled or scaled parameters, the water fluxes at the bottom of the profile may be underestimated.

Conclusions

In situ measurements of soil hydraulic properties lead to the best simulations of soil moisture dynamics, but labor, accessibility,

and cost issues preclude the conclusion that vadose zone investigations must include numerous colocated moisture and head measurements to facilitate inversion or direct measurement of the in situ moisture retention behavior. We found that the in situ moisture retention behavior at our study site was not well represented by laboratory MSO tests or commonly used PTFs, but that these measures or estimates could be dramatically improved by simply constraining the range of possible moisture contents by the minimum and maximum moisture contents measured in the field. It appears that this method of scaling PTF results can be used to obtain soil hydraulic property inputs of sufficient accuracy for plot-scale modeling efforts without requiring expensive laboratory or in situ tests. The next step is to validate the approach at other locations in the watershed and determine if these values can be scaled up for use in larger scale modeling efforts.

ACKNOWLEDGMENTS

We wish to thank J. Simunek for his assistance with the inverse modeling included in this work and J. Figueras and K. Unholz for running the MSO tests. This research was supported in part by the NSF-Idaho EPSCoR Program and the National Science Foundation under award no. EPS-0447689.

References

- ASTM. 2007. D422-63: Standard test method for particle-size analysis of soils. ASTM Int., West Conshohocken, PA.
- Basile, A., G. Ciollaro, and A. Coppola. 2003. Hysteresis in soil water characteristics as a key to interpreting comparisons of laboratory and field measured hydraulic properties. *Water Resour. Res.* 39(12):1355, doi:10.1029/2003WR002432.
- Blonquist, J.M., Jr., S.B. Jones, and D.A. Robinson. 2005. Standardizing characterization of electromagnetic water content sensors: Part 2. Evaluation of seven sensing systems. *Vadose Zone J.* 4:1059–1069.
- Bouwer, H., and R.C. Rice. 1983. Effect of stones on hydraulic properties of vadose zones. p. 77–93. *In* D.M. Nielsen and M. Curl (ed.) Proc. NWWA/USEPA Conf. on Characterization and Monitoring of the Vadose (Unsaturated Zone), Las Vegas, NV. 8–10 Dec. 1983. Natl. Well Water Assoc., Worthington, OH.
- Chanzy, A., M. Mumen, and G. Richard. 2008. Accuracy of top soil moisture simulation using a mechanistic model with limited soil characterization. *Water Resour. Res.* 44:W03432, doi:10.1029/2006WR005765.
- Clausnitzer, V., and J.W. Hopmans. 1995. Nonlinear parameter estimation: LM-OPT. General purpose optimization code based on the Levenberg–Marquardt algorithm. LAWR Rep. 100032. Univ. of California, Davis.
- Dane, J.H., and J.W. Hopmans. 2002. Hanging water column. p. 680–692. *In* J.H. Dane and G.C. Topp (ed.) *Methods of soil analysis. Part 4. Physical methods.* SSSA Book Ser. 5. SSSA, Madison, WI.
- Dane, J.H., and G.C. Topp. 2002. *Methods of soil analysis. Part 4. Physical methods.* SSSA Book Ser. 5. SSSA, Madison, WI.
- Feddes, R.A., P.J. Kowalik, and H. Zaradny. 1978. Simulation of field water use and crop yield. *Simulation Monogr.* PUDOC, Wageningen, the Netherlands.
- Figueras, J., and M.M. Gribb. 2009. Design of a user-friendly automated multi-step outflow apparatus. *Vadose Zone J.* 8:(in press).
- Flerchinger, G.L., C.L. Hanson, and J.R. Wright. 1996. Modeling evapotranspiration and surface energy budgets across a watershed. *Water Resour. Res.* 32:2539–2548.
- Green, C.T., D.A. Sontestrom, B.A. Bekins, K.C. Akstin, and M.S. Schulz. 2005. Percolation and transport in a sandy soil under a natural hydraulic gradient. *Water Resour. Res.* 41:W10414, doi:1029/2005WR004061.
- Gribb, M.M., R. Kodešová, and S.E. Ordway. 2004. Comparison of soil hydraulic property measurement methods. *J. Geotech. Geoenviron. Eng.* 130:1084–1095.
- Guan, H. 2005. Water above the mountain front: Assessing mountain-block recharge in semiarid mountainous regions. Ph.D. diss. New Mexico Inst. of Min. and Technol., Socorro.
- Klute, A., and C. Dirksen. 1986. Hydraulic conductivity and diffusivity: Laboratory methods. p. 687–729. *In* A. Klute (ed.) *Methods of soil analysis. Part*

1. Physical and mineralogical methods. 2nd ed. SSSA Book Ser. 5. SSSA, Madison, WI.
- Mallants, D., D. Jacques, P.-H. Tseng, M.Th. van Genuchten, and J. Feyen. 1997. Comparison of three hydraulic property measurement methods. *J. Hydrol.* 199:295–318.
- McNamara, J.P., D.G. Chandler, M. Seyfried, and S. Achet. 2005. Soil moisture states, lateral flow, and streamflow generation in a semi-arid, snow-driven catchment. *Hydrol. Processes* 19:4023–4038.
- Mualem, Y. 1976. A new model for predicting the hydraulic conductivity of unsaturated porous media. *Water Resour. Res.* 12:513–522.
- Pachepsky, Ya.A., D. Timlin, and G. Varallyay. 1996. Artificial neural networks to estimate soil water retention from easily measurable data. *Soil Sci. Soc. Am. J.* 60:727–733.
- Rawls, W.J., and D.L. Brakensiek. 1985. Prediction of soil water properties for hydrologic modeling. p. 293–299. *In* E.B. Jones and T.J. Ward (ed.) *Watershed management in the Eighties*. Proc. Irrig. Drain. Div., ASCE, Denver, CO. 30 Apr.–1 May 1985. Am. Soc. Civ. Eng., New York.
- Reynolds, W.D., D.E. Elrick, E.G. Youngs, H.W.G. Booltink, and J. Bouma. 2002. Saturated and field saturated water flow parameters. p. 802–816. *In* J.H. Dane and G.C. Topp (ed.) *Methods of soil analysis*. Part 4. Physical methods. SSSA Book Ser. 5. SSSA, Madison, WI.
- Richards, A.F. 1931. Capillary conduction of liquids through porous media. *Physics* 1:318–333.
- Schaap, M.G., F.L. Leij, and M.Th. van Genuchten. 1998. Neural network analysis for hierarchical prediction of soil hydraulic properties. *Soil Sci. Soc. Am. J.* 62:847–855.
- Schaap, M.G., F.J. Leij, and M.Th. van Genuchten. 2001. Rosetta: A computer program for estimating soil hydraulic parameters with hierarchical pedo-transfer functions. *J. Hydrol.* 251:163–176. Rosetta is available from the U.S. Salinity Lab. at www.ars.usda.gov/Services/docs.htm?docid=8953.
- Schaap, M.G., P.J. Shouse, and P.D. Meyer. 2003. Laboratory measurements of the unsaturated hydraulic properties at the Vadose Zone Transport Field Study Site. PNNL-14284. Pac. Northw. Natl. Lab., Richland, WA.
- Šimůnek, J., and M.Th. van Genuchten. 1996. Estimating unsaturated soil hydraulic properties from tension disc infiltrometer data by numerical inversion. *Water Resour. Res.* 32:2683–2696.
- Šimůnek, J., M.Th. van Genuchten, and M. Sejna. 2005. The HYDRUS-1D software package for simulating the movement of water, heat, and multiple solutes in variably saturated media. Version 3.0. HYDRUS Softw. Ser. 1. Dep. of Environ. Sci., Univ. of California, Riverside.
- Soil Survey Staff. 1975. *Soil Taxonomy: A basic system of soil classification for making and interpreting soil surveys*. Agric. Handbk. 436. U.S. Gov. Print. Office, Washington, DC.
- Thomasson, M.J., P.J. Wierenga, and T.P.A. Ferre. 2006. A field application of the scaled-predictive method for unsaturated soil. *Vadose Zone J.* 5:1093–1109.
- van Genuchten, M.Th. 1980. A closed-form equation for predicting the hydraulic conductivity of unsaturated soils. *Soil Sci. Soc. Am. J.* 44:892–898.
- van Genuchten, M.Th. 1987. A numerical model for water and solute movement in and below the root zone. Res. Rep. 121. U.S. Salinity Lab., Riverside, CA.
- van Genuchten, M.Th., F.J. Leij, and S.R. Yates. 1991. The RETC code for quantifying the hydraulic functions of unsaturated soils. Version 1.0. USEPA Rep. 600/2–91/065. USSL, USDA, ARS, Riverside, CA. The RETC code is available from the USEPA at www.epa.gov/ada/csmos/models/retc.html.
- Vogel, T., M.Th. van Genuchten, and M. Cislérova. 2000. Effect of the shape of the soil hydraulic functions near saturation on variably-saturated flow predictions. *Adv. Water Resour. Res.* 24:133–144.
- Watson, K.K. 1966. An instantaneous profile method for determining the hydraulic conductivity of unsaturated porous materials. *Water Resour. Res.* 2:709–715.
- Williams, C.J. 2005. Characterization of the spatial and temporal controls on soil moisture and streamflow generation in a semi-arid headwater catchment. M.S. thesis. Boise State Univ., Boise, ID.
- Williams, C.J., J.P. McNamara, and D.G. Chandler. 2008. Controls on the spatial and temporal variation of soil moisture in a mountainous landscape: The signatures of snow and complex terrain. *Hydrol. Earth Syst. Sci. Discuss.* 5:1927–1966.
- Wösten, J.H.M., A. Lilly, A. Nemes, and C. Le Bas. 1999. Development and use of a database of hydraulic properties of European soils. *Geoderma* 90:169–185.
- Wösten, J.H.M., Ya.A. Pachepsky, and W.J. Rawls. 2001. Pedotransfer functions: Bridging the gap between available basic soil data and missing soil hydraulic characteristics. *J. Hydrol.* 251:123–150.
- Ye, M., R. Khaleel, M.G. Schaap, and J. Zhu. 2007. Simulation of field injection experiments in a layered formation using geostatistical methods and artificial neural network. *Water Resour. Res.* 43:W07413, doi:10.1029/2006WR005030.